boom was kept constant at some value, and the length of the boom was varied, thus resulting in an inertia change. The results obtained here were similar to those observed for boom mass change. Damper performance can be greatly enhanced by using very long booms, but there is a limit to admissible boom length both from the practical point of view as well as the point of view of system performance. We also found that changes in boom length had a much more dramatic impact on damper performance than changes in boom mass.

Finally, we assessed the ability of one of the booms to reduce nutation in the event of a malfunction of the other. As expected, one boom was not as effective as the two-boom system in damping out nutation. Nutation damper time constant values increased for each given spring stiffness and for all values of the damping factor. However, the performance still remained quite reasonable. For example, assuming a spring stiffness of 300 N-m/rad and a damping factor of 2500 N-m-s/rad (values close to those used on the Galileo spacecraft), the time constant only increased to about 3 min when only one damper was functional. It is thus apparent that spacecraft nutation can still be kept under control even if one of the boom dampers should malfunction.

Conclusion

This study is motivated by the fact that many spacecraft carry rod-like attachments, which are usually rigidly connected to the spacecraft's main bus and which are used as antennas or for various other purposes during the spacecraft's mission. The study investigates the idea of converting any two of such rod-like elements into pendulous dampers for the purpose of controlling nutation for spinning spacecraft. The study is restricted to the case where the two booms that are converted to dampers are identical and placed symmetrically with respect to the spacecraft's main body and where the rigid inner body is a major axis spinner. The results obtained demonstrate that the proposed arrangement has great merit for several reasons. The rate at which nutation is damped by the proposed dual-damper system is found to be relatively insensitive to such system parameters as the device's damping factor. This is a major advantage over traditional dampers, for which tuning is normally a necessity. From a practical point of view, the fact that the damping factor can vary widely without much degradation in performance can lead to a much simpler physical device for the system's dashpot. For example, there will be no need to include elaborate temperature control systems that would ordinarily be needed to keep the temperature (and thus the damping factor) of the damper fluid within a tight band.

This study also shows that the performance of the damper system is influenced by the length of the booms, as well as by the ratio of the mass of the booms to that of the whole spacecraft. Each of these has a limiting value, below which an increase in the parameter improves performance and above which the reverse is the case. These limiting values depend on the spin rate of the spacecraft; they are lowered by increasing the spin rate. In general, changes in boom length have a more dramatic influence on damper effectiveness than changes in boom mass. Finally, the proposed arrangement naturally introduces redundancy into the nutation control scheme. Failure of one of the boom dampers does not constitute a crisis because the second damper can continue with the nutation damping process at a reasonable rate.

Acknowledgment

This material is based upon work supported in part by NASA under award NAG-2-4003.

References

[1] Iorillo, A. J., "Nutation Damping Dynamics of Rotor Stabilized Satellites," American Society of Mechanical Engineers Winter Meeting, Chicago, Nov. 1965.

[2] Likins, P. W., "Attitude Stability Criteria for Dual-Spin Spacecraft," *Journal of Spacecraft and Rockets*, Vol. 4, No. 12, 1967, pp. 1638–1643.

[3] Auelmann, R. R., and Lane, P. T., "Design and Analysis of Ball-in-Tube Nutation Dampers," *Proceedings of the Symposium on Attitude Stabilization and Control of Dual-Spin Spacecraft*, Air Force Rept. SAMSO-TR-68-191, 1968, pp. 81–90.

[4] Spencer, T. M., "Cantilevered-Mass Nutation Damper for Dual-Spin Spacecraft," *Proceedings of the Symposium on Attitude Stabilization and Control of Dual-Spin Spacecraft*, Air Force Rept. SAMSO-TR-68-191, 1968, pp. 91–109.

[5] Taylor, R. S., and Conway, J. J., "Viscous Ring Precession Damper for Dual-Spin Spacecraft," *Proceedings of the Symposium on Attitude Stabilization and Control of Dual-Spin Spacecraft*, Air Force Rept. SAMSO-TR-68-191, 1968, pp. 75–80.

[6] Yeates, C. M., and Clark, T. C., "The Galileo Mission to Jupiter," *Astronomy*, Vol. 10, No. 1, 1982.

[7] Rasmussen, R. D., and Brown, T. K., "Attitude and Articulation Control Solutions for Project Galileo," Paper 80-019, American Astronautical Society, Feb. 1980.

[8] Bernard, D., "Passive Nutation Damping Using Large Appendages with Application to Galileo," *Journal of Guidance, Control, and Dynamics*, Vol. 5, No. 2, 1982, pp. 174–180.

[9] McIntyre, J. E., and Miyagi, M. I., "A General Stability Principle for Spinning Flexible Bodies with Application to the Propellant Migration-Wobble Amplification Effect," *Proceedings of a Symposium on Dynamics and Control of Non-Rigid Spacecraft*, European Space Agency, 1976, pp. 159–175.

[10] Kane, T. R., and Levinson, D. A., *Dynamics On Line*, OnLine Dynamics, Palo Alto, CA, 1996, pp. 197–257.

Frequency-Domain Recursive Robust Identification

Xu Feng* and Ching-Fang Lin†
American GNC Corporation, Chatsworth, California 91311
and
Norman P. Coleman‡
Army Armament Research, Development and Engineering Center, Picatinny Arsenal, New Jersey 07806

I. Introduction

CONVENTIONAL system identification theory is mainly focused on how to obtain a single accurate model of the plant and how to ensure that the obtained model approaches the real model of the plant. It is assumed that the best an identification algorithm can provide is a good model that is sufficiently close to the real model. For controller design purposes, this assumption implies that a controller, which is designed for a good model, will exhibit good performance when it is applied to the real plant. Such an assumption has been widely used in control practice.[1]

Recently, alternative approaches to system identification for controller design have been proposed.[2–5] One of the alternatives is to derive a family of models instead of a single model to ensure that the true dynamics of the plant are included in the model family. Obviously, this is a more practical approach than conventional ones, especially for those plants with highly complex dynamics, such as aerospace systems.

In this Note, a frequency-domain recursive robust identification algorithm is proposed for a system with unmodeled dynamics. The algorithm yields estimates of the system transfer function at N frequency points on the unit circle, as well as the error bounds of these estimates. Such estimation results provide potential data for the so-called H_∞ identification approaches, which in turn provide possible models for the robust (H_∞) controller design.[5]

Received 8 January 1998; revision received 15 April 1999; accepted for publication 18 April 2000.

*Senior Research Scientist, 9131 Mason Avenue; xfeng@americangnc.com.

†President, 9131 Mason Avenue; cflin@americangnc.com. Associate Fellow AIAA.

‡Chief, Automation and Robotics Laboratory, AMSTA-AR-FSF-R; ncoleman@pica.army.mil.

II. Problem Formulation

In the context of system identification, available data usually lie in the time domain. To obtain the estimation of the unstructured uncertainty in the frequency domain, the data in the time domain will be mapped into the frequency domain appropriately.[2]

For simplicity, consider a single-input/single-output (SISO) discrete-time system

$$y_n = G(q^{-1})u_n \tag{1}$$

where q^{-1} is the delay operator. System uncertainty is described by

$$G(z) = G_0(z) + \Delta(z)D(z) \tag{2}$$

where $G_0(z)$ is a stable and time-invariant nominal model. $\Delta(z)D(z)$ represents the unstructured uncertainty, where $D(z)$ is the bound of the unstructured uncertainty, which is also stable and time invariant; $\Delta(z)$ characterizes the unknown dynamics of the system and is subject to the constraint that the l_1 norm of $\Delta(z)$ is bounded by 1, that is,

$$\sum_{i=0}^{\infty} |h_{\Delta,i}| \le 1$$

where $\{h_{\Delta,i}, i = 0, 1, \ldots\}$ is the unit pulse response series of $\Delta(z)$. Assume that the following are known *a priori*: 1) known constants $M_0 > 0$, $\rho_0 > 1$, $M_D > 0$, and $\rho_D > 1$, such that the unit pulse responses of $G_0(z)$, $D(z)$ satisfy $|h_{0,i}| \le M_0\rho_0^{-i}$ and $|h_{D,i}| \le M_D\rho_D^{-i}$, $i = 0, 1, \ldots$; 2) a known parameter $u_{\max}$, where $u_{\max} = \sup_i |u_i|$; and 3) zero initial condition, that is, $u_i = 0$ and $y_i = 0$, when $i < 0$.

Our objective is to derive a finite number of frequency point estimates of the transfer function on the unit circle and their associated error bounds based on the *a priori* information.

Minimal *a priori* information is assumed because it only consists of a lower bound on the relative plant stability, an upper bound on a certain plant gain, and an upper bound on the input signal. Particularly, no assumptions are made concerning the structure of the plant.

III. Frequency Point Estimates and Related Error Bounds

The discrete Fourier transformation (DFT) is exploited to convert the input–output data in the time–domain into the frequency point estimates in the frequency domain. Define $Y_{N,n}(\omega_k)$, the N point DFT of the output signal, with length N, that ends at n,

$$Y_{N,n}(\omega_k) = \sum_{m=n-N+1}^{n} y_m W_N^{km}, \qquad k = 0, 1, \ldots, N-1 \tag{3}$$

where $\omega_k = 2\pi k/N$, $W_N = \exp(-2\pi j/N)$. $U_{N,n}(\omega_k)$ is defined similarly for the input signal.

Theorem 1: For the system described by Eqs. (1) and (2), the following relationship holds

$$Y_{N,n}(\omega_k) = G\{\exp[j(2\pi k/N)]\}U_{N,n}(\omega_k) + E_{N,n}(\omega_k)$$

$$k = 0, 1, \ldots, N-1 \tag{4}$$

where

$$E_{N,n}(\omega_k) = \sum_{i=1}^{\infty} h_{0,i} W_N^{ki}[U_{N,n-i}(\omega_k) - U_{N,n}(\omega_k)]$$

$$+ \Delta(q^{-1})D(q^{-1})U_{N,n}(\omega_k) - \Delta\left[\exp\left(j\frac{2\pi k}{N}\right)\right]$$

$$\times D\left[\exp\left(j\frac{2\pi k}{N}\right)\right]U_{N,n}(\omega_k) \tag{5}$$

Furthermore, there exists a positive integer L such that $E_{N,n}(\omega_k)$ is bounded by $\bar{E}_{N,n}(\omega_k)$, that is,

$$|E_{N,n}(\omega_k)| \le \bar{E}_{N,n}(\omega_k) = \sum_{i=1}^{L-1} M_0\rho_0^{-i}|U_{N,n-i}(\omega_k) - U_{N,n}(\omega_k)|$$

$$+ 2u_{\max}M_0\rho_0^{-L+1}\frac{L\rho_0 - L + 1}{(\rho_0 - 1)^2} + 2u_{\max}M_D\rho_D\frac{N}{(\rho_D - 1)} \tag{6}$$

Theorem 1 is applied to derive the following frequency point estimates and related error bounds from Eqs. (4) and (6),

$$|G\{\exp[j(2\pi k/N)]\} - G_{N,n}(\omega_k)| \le R_{N,n}(\omega_k)$$

$$k = 0, 1, \ldots, N-1 \tag{7}$$

$$G_{N,n}(\omega_k) = \frac{Y_{N,n}(\omega_k)}{U_{N,n}(\omega_k)}, \qquad R_{N,n}(\omega_k) = \frac{\bar{E}_{N,n}(\omega_k)}{|U_{N,n}(\omega_k)|} \tag{8}$$

Equation (7) provides a recursive algorithm that is able to provide N frequency point estimates of the transfer function on the unit circle. Interpreting Eq. (7) as N disks in the complex plane that are centered at $G_{N,n}(\omega_k)$ with radii $R_{N,n}(\omega_k)$, the true values of the transfer function at these frequency points are guaranteed to be within these disks. Generally, disks derived at different times are different. It is in this sense that an updating mechanism is necessary to improve accuracy. A simple approach to update the estimates is to choose the disk with the smallest radius as the latest estimate, as adopted by LaMaire et al.[2] The result of this approach is that only the information contained in the sizes of the disks is utilized and no attention is paid to the positions of the disks. To utilize the information stored in the positions of the disks, it is helpful to study the geometric relationship between two successive estimates, as in Fig. 1.

Theorem 2: Let two disks be given, described by

$$\boldsymbol{C}_1: (x - x_1)^2 + (y - y_1)^2 \le R_1^2$$

$$\boldsymbol{C}_2: (x - x_2)^2 + (y - y_2)^2 \le R_2^2 \tag{9}$$

If they overlap, the disk that merely covers the overlapped area can be determined by

$$\left(x - \frac{x_1 + \gamma x_2}{1 + \gamma}\right)^2 + \left(y - \frac{y_1 + \gamma y_2}{1 + \gamma}\right)^2 \le R(\gamma) \tag{10}$$

$$R(\gamma) = \frac{(1+\gamma)R_1^2 + (\gamma + \gamma^2)R_2^2 - \gamma(x_1 - x_2)^2 - \gamma(y_1 - y_2)^2}{(1+\gamma)^2} \tag{11}$$

$$\gamma = \frac{(x_1 - x_2)^2 + (y_1 - y_2)^2 + R_1^2 - R_2^2}{(x_1 - x_2)^2 + (y_1 - y_2)^2 + R_2^2 - R_1^2} \tag{12}$$

By the utilization of Theorem 2 as the updating algorithm, the error bound is guaranteed to be monotonically decreasing by design, because the size of the disk that only covers the intersection of the two disks is always smaller than that of either of these two disks. Furthermore, the two parameters $R(\gamma)$ and γ are indicative of the relative position of the two disks, as shown in Fig. 2. In the following,

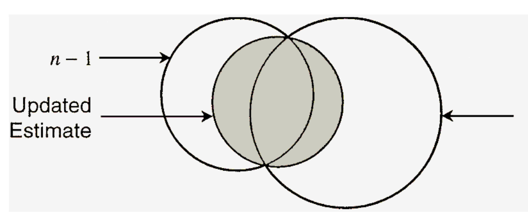

Fig. 1 Geometric relationship.

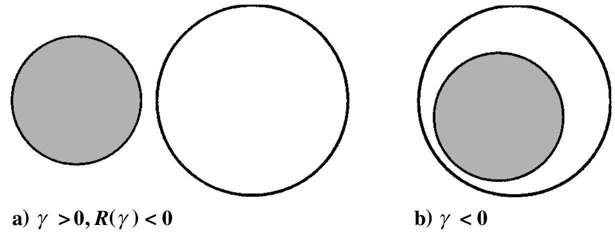

a) $\gamma > 0, R(\gamma) < 0$ **b)** $\gamma < 0$

Fig. 2 Relative position.

we summarize the recursive identification algorithm for frequency point estimates, based on Theorems 1 and 2:

1) Compute the parameter γ that is indicative of the relative position of the two disks,

$$\gamma = \frac{|\bar{G}_n(k) - G_{N,n+1}(\omega_k)|^2 + \bar{E}_n(k)^2 - R_{N,n+1}(\omega_k)^2}{|\bar{G}_n(k) - G_{N,n+1}(\omega_k)|^2 - \bar{E}_n(k)^2 + R_{N,n+1}(\omega_k)^2}$$

2) If $\gamma \leq 0$, the estimate and error bound are updated by

$$\bar{G}_{n+1}(k) = \begin{cases} \bar{G}(k), & \text{if} \quad \bar{E}_n(k) \leq R_{N,n+1}(\omega_k) \\ \bar{G}_{N,n+1}(\omega_k), & \text{if} \quad \bar{E}_n(k) > R_{N,n+1}(\omega_k) \end{cases}$$

$$\bar{E}_{n+1}(k) = \min\{\bar{E}_n(k), R_{N,n+1}(\omega_k)\}$$

3) If $\gamma > 0$, first compute the parameter $R(\gamma)$ that is indicative of the size of the disk that only covers the intersection of the two disks,

$$R(\gamma) = \left[(1+\gamma)\bar{E}_n(k)^2 + (\gamma + \gamma^2)R_{N,n+1}(\omega_k)^2 - \gamma|\bar{G}_n(k) - G_{N,n+1}(\omega_k)|^2\right]\big/(1+\gamma)^2$$

Then update the estimate and error bound. If $R(\gamma) \geq 0$, they are updated by

$$\bar{G}_{n+1}(k) = [\bar{G}_n(k) + \gamma G_{N,n+1}(\omega_k)]/(1+\gamma)$$

$$\bar{E}_{n+1}(k) = \sqrt{R(\gamma)}$$

If $R(\gamma) < 0$, the updating rule is

$$\bar{G}_{n+1}(k) = \tfrac{1}{2}[\bar{G}_n(k-1) + \bar{G}_n(k+1)]$$

$$\bar{E}_{n+1}(k) = \tfrac{1}{2}[\bar{E}_n(k-1) + \bar{E}_n(k+1)]$$

IV. Illustrative Simulation

In this section, the recursive robust identification algorithm is demonstrated through a simple illustrative example. Consider the uncertain discrete-time system

$$G(z) = \frac{0.39347}{z - 0.60653} + \Delta(z)\frac{0.001z}{z - 0.36788}$$

The nominal system is obtained by discretizing the continuous system $1/(s+1)$ with a sampling period of 0.5 s and passing it through a zeroth-order hold. For this system, $M_0 = 0.39347/0.60653 = 0.64872$, $\rho_0 = 1/0.60653 = 1.6487$, $M_D = 0.001$, and $\rho_D = 1/0.36788 = 2.7183$. To generate the input–output data in the simulation, the unknown factor $\Delta(z)$ is set to be $\Delta(z) = 0.55065\, z/(z - 0.44933)$, which satisfies

$$\sum_{i=0}^{\infty} |h_{\Delta,i}| \leq \frac{0.55065}{1.0 - 0.44933} = 0.99996 < 1.0$$

The input signal is chosen to be $u(n) = \sin(\pi n/5)$. To test the robustness of the algorithm, Gaussian noise is added to the system output with a distribution of $N(0, 0.2)$. Setting $N = 128$ and $L = 20$, the algorithm in Sec. III is applied to the generated simulation data to estimate the nominal model and its associated uncertainty bound. The result when $n = 120$ is shown in Fig. 3. For comparison, the results from the algorithm by LaMaire et al.[2] are also shown. It is clear that our algorithm produces a much tighter uncertainty bound. To show how the error bounds converge during iteration, Fig. 4 shows the convergence of the error bound at $\omega_k (k = 0)$. As is clearly shown, the error bound of our algorithm is monotonically decreasing and converges to a much lower error bound than the algorithm by LaMaire et al.[2]

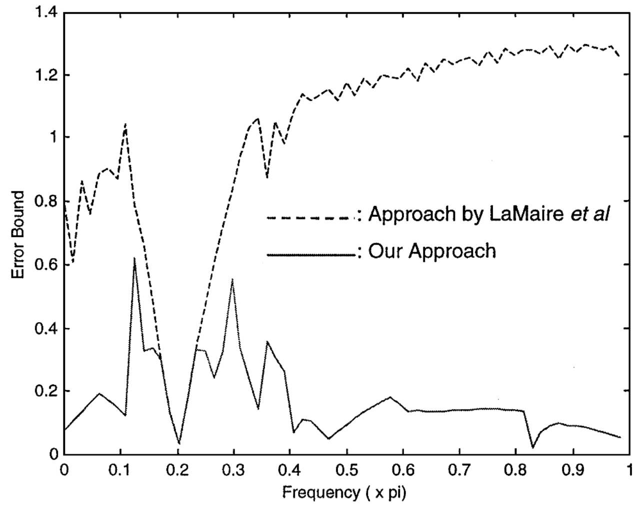

Fig. 3 Comparison of error bounds.

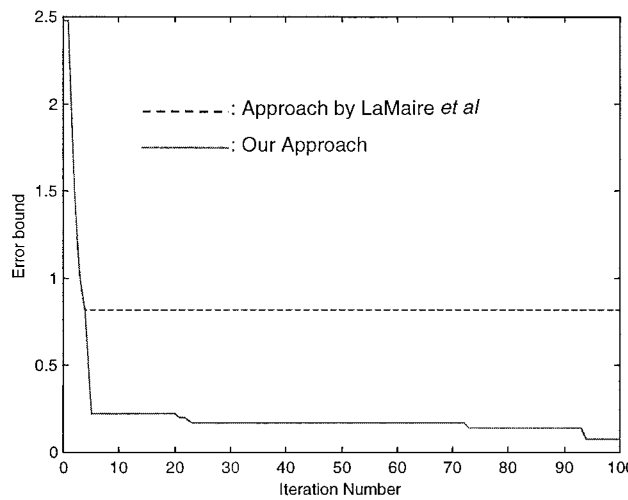

Fig. 4 Convergence of error bound.

V. Conclusions

The algorithm proposed in this Note is basically a robust identification algorithm based on the nonparametric model.[4] For a system with unmodeled uncertainty, the algorithm yields estimates of the system transfer function at N frequency points, as well as the error bounds of these estimates. Such estimation results provide potential data for the H_∞ identification approaches, which in turn provide possible models for the robust (H_∞) controller design.

References

[1] Lin, C. F., *Advanced Control System Design*, Prentice–Hall, Englewood Cliffs, NJ, 1993, Chap. 19.

[2] LaMaire, R. O., Valavani, L., Athans, M., and Stein, G., "A Frequency-Domain Estimator for Use in Adaptive Control Systems," *Automatica*, Vol. 27, No. 1, 1991, pp. 23–38.

[3] Bayard, D. S., Hadeagh, F. Y., Yam, Y., Scheid, R. E., Mettler, E., and Milman, M. H., "Automated On-Orbit Frequency Domain Identification for Large Space Structures," *Automatica*, Vol. 27, No. 6, 1991, pp. 931–946.

[4] Feng, X., and Sun, Y. X., "A Survey on Robust Identification Problem," *Control Theory and Applications*, Vol. 10, No. 6, 1993, pp. 609–616.

[5] Helmicki, A. J., Jacobson, C. A., and Nett, C. N., "Control Oriented System Identification: a Worst-Case/Deterministic Approach in H_∞," *IEEE Transactions on Automatic Control*, Vol. 36, No. 10, 1991, pp. 1163–1176.